Received: 1 September 2016 | Accepted: 9 January 2017

DOI: 10.1111/jace.14792

ORIGINAL ARTICLE

Journal of the American Ceramic Society

Microstructural evolution in infiltration-growth processed MgB_2 bulk superconductors

Ashutosh G. Bhagurkar[1] | Akiyasu Yamamoto[2] | Anthony R. Dennis[3] | John H. Durrell[3] | Talal A. Aljohani[4] | Hari B. Nadendla[1] | David A. Cardwell[3]

[1]Brunel Centre for Advanced Solidification Technology, Brunel University London, Uxbridge, UK

[2]Department of Applied Physics, Tokyo University of Agriculture and Technology, Tokyo, Japan

[3]Bulk Superconductivity Group, Department of Engineering, University of Cambridge, Cambridge, UK

[4]National Centre for Advanced Materials, King Abdulaziz City for Science and Technology, Riyadh, Saudi Arabia

Correspondence
Ashutosh G. Bhagurkar, Brunel Centre for Advanced Solidification Technology, Brunel University London, Uxbridge, UK.
Email: ashutosh.bhagurkar@brunel.ac.uk

Funding information
KACST-Cambridge Joint Centre of Excellence in Advanced Materials and Manufacturing; Engineering and Physical Sciences Research Council, Grant/Award Number: EP/K031422/1.

Abstract

The study reports phase and microstructural evolution in MgB_2 bulk superconductors fabricated by an infiltration and growth (IG) process. Three distinct stages, (1) intermediate boride formation, (2) bulk liquid Mg infiltration, and (3) MgB_2 layer formation, were identified in IG process after detailed examination of series of samples prepared with varied heating conditions. The intermediate phase Mg_2B_{25}, isomorphous to β-boron, was detected prior to MgB_2 phase formation in stage (1). Due to volume expansion involved in stage 1, cracks formed in the β-boron particles and propagated radially inwards during stage 3. The growing MgB_2 particles sintered simultaneously with formation of grain boundaries during the process, as evidenced by the measured hardness and critical current density in these samples. From our observations, we estimate the total time needed for complete transformation to MgB_2.

KEYWORDS
infiltration and growth, MgB_2, superconductors

1 | INTRODUCTION

Superconducting MgB_2 is an exciting candidate for practical applications due to a relatively high T_c (39 K), low raw material cost, low density (2.6 g/cm^3), ease of fabrication, and the absence of any deleterious effect on critical current arising from grain boundaries.[1,2] Infiltration and growth (IG) is a promising route for the fabrication of MgB_2 bulk superconductors, typically involving impregnation of liquid magnesium, Mg(l), into a porous solid boron, B(s), preform. The resultant product is essentially a MgB_2-Mg ceramic matrix composite, with Mg levels up to 15%. The relative density of IG processed MgB_2 is significantly higher (>90%) than samples fabricated using conventional sintering techniques, with process requiring no high-pressure apparatus.[3,4] Moreover, near-net complex shapes can be fabricated with infiltration route that are not easily achievable by conventional sintering methods.[5,6]

Although significant advances have been made to the IG process to enable fabrication of high-quality bulk samples,[5,7,8] only a few reports have commented on underlying mechanism of the process. Notably, DeFouw et al.[9] proposed a diffusion based model for MgB_2 growth in boron fibers. They observed radial and circumferential growth of MgB_2, via the formation of intermediate phases, including MgB_7 and MgB_4. Radial growth of the MgB_2 phase occurred mainly due to the formation of radial cracks due

to an associated volume expansion. Similarly, Albisetti et al. suggested that Mg_2B_{25} could be a precursor to MgB_2 formation in RLI process through analysis of various reactive liquid infiltration (RLI) processed samples.[10] More recently, Li et al.[11] have suggested that the thickness of the first layer of MgB_2 formed at the Mg(l)-B(s) interface is critical in determining the overall fraction of MgB_2 in the final reacted IG processed MgB_2 wires. They accounted for this as being due to the fact that Mg atoms needed to diffuse through the MgB_2 layer in order to react with the B.

For this study, we devised experiments aimed at understanding the growth mechanism of the superconducting MgB_2 phase during the IG process. The resultant microstructural evolution in the samples is discussed via the analysis of series of samples. Finally, we propose a possible mechanism for the growth of superconducting MgB_2.

2 | EXPERIMENTAL PROCEDURE

Crystalline β-boron (98% pure, HC Starck, <40 μm; Karlsruhe, Germany), weighing 1.5 g, was pressed uniaxially into cylindrical precursor pellets of diameter 16 mm and thickness 6 mm under a load of 20 MPa. SEM images (not shown here) of β-B powder suggested a bimodal particle size distribution with most particles with sizes of 5-10 μm and ~30 μm. A total of 10 such boron precursors were prepared. The IG process was performed as follows- The pressed precursor pellets were placed in a perforated steel enclosure and the entire assembly was introduced in crucible containing liquid Mg at 750°C. $N_2 + SF_6$ (volume ratio 95:5) cover gas was maintained above Mg melt surface to minimize oxidation of Mg. SF_6 gas is known to react with Mg(l) to form MgF_2, which fills the pores in otherwise porous MgO film on the melt surface.[12] The temperature of the melt was then raised to a target temperature at 300°C/h. At the end of holding time, temperature of the melt was reduced to 750°C and steel enclosure containing IG processed MgB_2 sample was recovered from the liquid Mg bath.[13] This procedure slightly varies from reactive liquid infiltration method adopted by Giunchi et al., where Mg bulk and B precursor were placed in a metallic container. It was later welded prior to heat treatment to obtain dense, bulk MgB_2.[4] Seven of the B precursors were subjected to IG process at fixed temperature of 750°C for durations of 5 minutes, 10 minutes, 20 minutes, 40 minutes, 1 hour, 2 hours, and 4 hours. To study the influence of reaction temperature, the remaining three precursors were reacted with a constant soaking time of 4 hours and varying reaction temperatures of 800°C, 850°C, and 900°C. The reacted product from IG process, when in the form of hard bulk, was slightly ground to remove Mg metal on bulk surface. Wherever powdery reacted product was obtained, especially for soaking time <20 minutes, all the powder was carefully collected. Weight of all the samples were recorded to estimate Mg intake, since weight of starting B precursor was kept constant at 1.5 g. The samples were then characterized using various physical property and compositional measurement techniques such as scanning electron microscopy (SEM), X-ray diffraction (XRD), and Vickers hardness measurements. The critical current densities (J_c) of these samples were calculated from measured magnetic moment hysteresis loops using the extended Bean model for a rectangular cross section in a perpendicular, applied magnetic field.[14]

3 | RESULTS

From our observations, we divide the overall growth of superconducting MgB_2 in the IG process into three stages:

3.1 | Stage 1: Initiation of cracks in the boron particle: Mg_2B_{25} phase formation process

The SEM images of samples reacted isothermally at 750°C at 5 minutes, 10 minutes, 20 minutes, and 40 minutes are shown in Figures 1A,B,C,D, respectively. The sample reacted for 5 minutes is observed to be free from Mg with no sign of phase transformation. The sample reacted for 10 minutes, however, shows initiation of cracks in some of the particles (indicated in Figure 1 by green dashed circles), whereas almost all the B particles in sample reacted for 20 minutes show radially inward multiple cracks, exposing fresh B region to Mg vapor. The XRD patterns of these samples, shown in Figure 2, reveal an increasing appearance of Mg_2B_{25}, a recently discovered phase, in sample reacted for 10 and 20 minutes, suggesting a strong correlation between cracking and transformation of β-rhombohedral into Mg_2B_{25}.[15,16] This is illustrated as stage 1 in schematic of IG process in Figure 3.

3.2 | Stage 2: Mg uptake in the porous precursor

The overall weight gain in the precursor as a function of reaction time at a fixed temperature (750°C), plotted in Figure 4, enables the study of rate of influx of Mg with time (Figure 3, Stage 2). Given that XRD did not detect any traces of MgO (Figure 2), all the gain in weight of the sample can be attributed to liquid Mg only. Mg uptake into the precursor pellet could only be observed after 40 minutes of reaction. Samples reacted for 5, 10, and 20 minutes showed no detectable weight gain. Conversely, the sample reacted for 40 minutes showed an 80% weight gain while the 1 hour sample exhibited a doubling in weight. It is

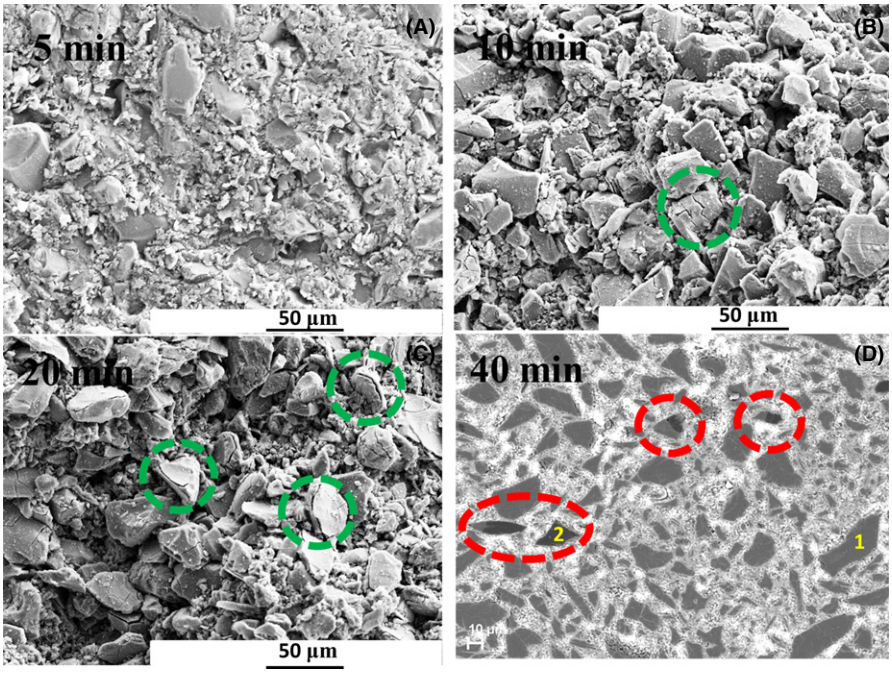

FIGURE 1 SEM images of samples reacted at 750°C for 5, 10, 20, and 40 minutes, respectively

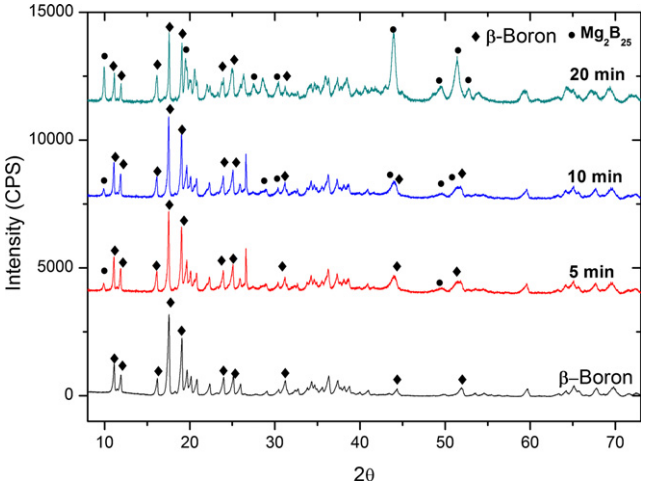

FIGURE 2 XRD patterns for the samples reacted for 5, 10, and 20 minutes, respectively, at 750°C. Plot for β-boron also shown for comparison

noted that doubling (100% weight gain-1.5 g Mg) also satisfies the stoichiometric requirement of the quantity of Mg needed to react with B in the precursor. The sample reacted for longer than 1 hour showed no further uptake of Mg.

3.3 | Stage 3: Transformation of Mg_2B_{25} to MgB_2: rate determining step

The following three phenomena are observed concurrently in the final stage IG process.

3.3.1 | Propagation of primary cracks in Mg_2B_{25} particles and fragmentation

Figures 5A,B show back scatter electron images of samples reacted at 750°C for 40 minutes and 2 hours, respectively. The sample reacted for 40 minutes shows the presence of Mg(l) (bright in contrast) within pores in the precursor and radial cracks that formed during Stage 1 (as shown by black arrows). It is quite apparent that cracks in the sample reacted for 2 hours are deeper in to the particle than that of particles in the sample reacted for 40 minutes. These cracks propagated through the Mg_2B_{25} particle, and even extend throughout the entire particle cross section, as can be seen from Figure 5B. Consequently, these cracks resulted in fracture and fragmentation in some of the particles indicated by red dashed circles). During Isothermal heat treatment at 750°C. XRD analysis (not shown here) indicates that samples reacted at 750°C for 40 minutes and 2 hours contained Mg_2B_{25} phase of up to 40% and 30% (volume), respectively.

3.3.2 | Diffusion-controlled MgB_2 growth

Figures 6A,B compare the microstructures of samples reacted for 4 hours at 750°C and 900°C, respectively. High residual Mg content and a large amount of Mg_2B_{25} phase is present in the sample reacted at 750°C. The sample reacted for 900°C shows large depth of MgB_2 layer thickness on individual particle or "diffusion zone", indicating the Mg diffusion distance into Mg_2B_{25} particle. Moreover, smaller particles of size 5 µm appear to have completely

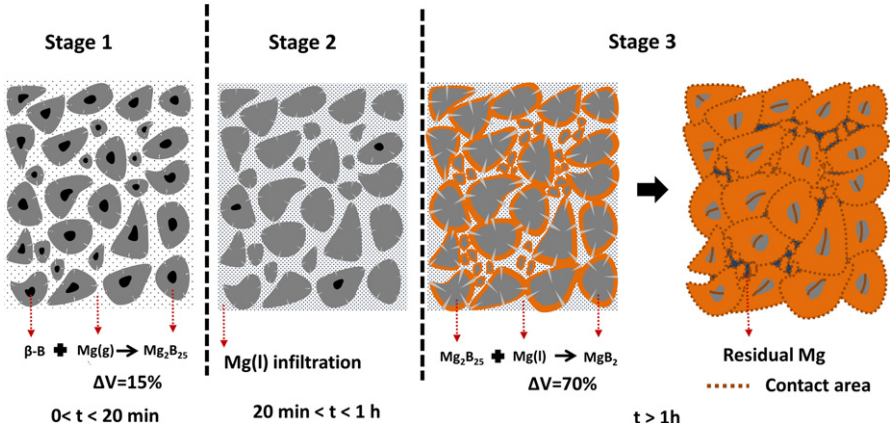

FIGURE 3 Schematic illustration of microstructure and phase evolution during the IG process

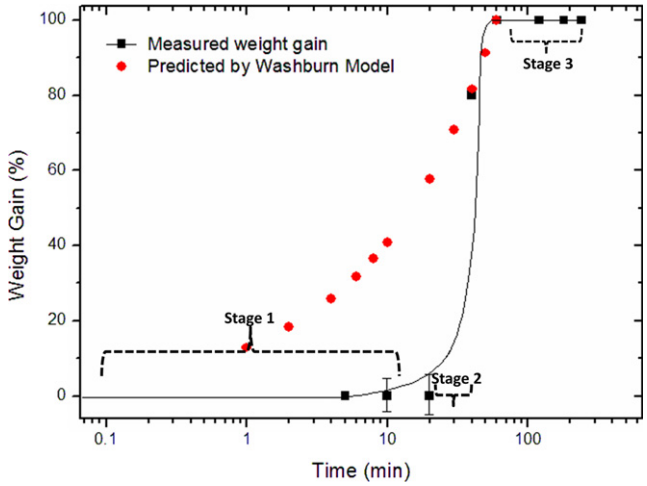

FIGURE 4 Measured weight gain in IG sample compared with that predicted by classical capillary infiltration, as a function of reaction time. The 5% error for samples reacted for 10 and 20 minutes accounts for losses associated with the handling of powdery, reacted product

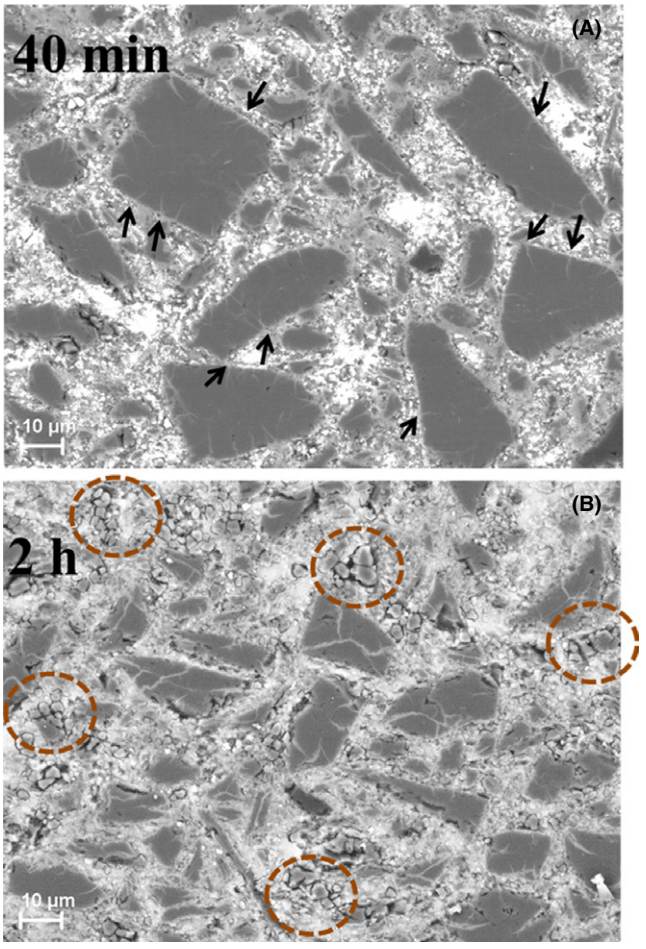

FIGURE 5 SEM images of IG processed samples. (A) The sample reacted for 40 minutes shows smaller crack length (shown by arrows). (B) The sample reacted for 2 h shows propagation of cracks and ultimate fracture in Mg_2B_{25} particles (indicated by dotted circles)

transformed into a different phase. XRD patterns and the corresponding estimated phase contents at each temperature (750°C, 800°C, 850°C, and 900°C) are shown in Figures 7A,B, respectively. Phase content of Mg_2B_{25} and Mg at 750°C is estimated to be about ~26% and 33%, respectively. It is reduced progressively as the temperature increases and reaches ~12% and 14%, respectively, at 900°C, which clearly suggests that growth of superconducting MgB_2 phase occurs at the expense of Mg_2B_{25} and Mg phase consumption.

3.3.3 | Simultaneous sintering

Figure 8 shows the variation in bulk hardness and critical current density as a function of reaction temperature. It is evident that critical current density increases with the reaction temperature. The growth of MgB_2 occurs radially inwards in the boron particles and this superconducting

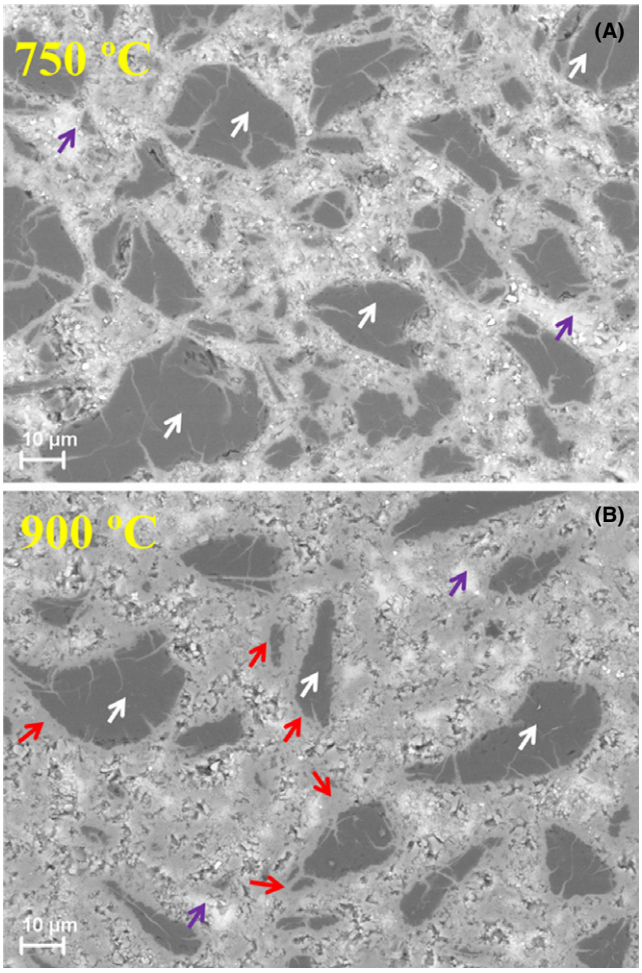

FIGURE 6 SEM images of samples reacted for 4 h at (A) 750°C and (B) 900°C. The red arrows indicate the "Diffusion zone". The purple arrows indicate unreacted Mg and the white arrows indicate the Mg_2B_{25} phase

layer undergoes almost twofold volume expansion. These growing particles impinge on one another and sinter simultaneously (Figure 3, Stage 3), as evident in our previous studies[6]. The sintering process enhances the grain connectivity and is responsible for the observed increased J_c as a function of soaking temperature. Increased hardness as a function of temperature also suggests increased grain connectivity by the sintering process.

4 | DISCUSSION

It is clear from Stage 1 that Mg_2B_{25} is a nonequilibrium intermediate phase in the MgB_2 phase formation and is also stable at room temperature. The crystal structure of the Mg_2B_{25} phase can be described as partial occupancy of Mg atoms (7.4 atomic %) at interstitial sites (namely A, D, E, and F) in a complex rhombohedral unit cell of β-boron comprising of 105 atoms. Thus, major structural rearrangement of β-boron is not necessary, although lattice constants are slightly enhanced.[15,16] Given that the influx of Mg(l) is below detectable limits in the initial stages of the infiltration process, it is likely that the Mg atoms that are transported from liquid source to individual β-boron particles to form Mg_2B_{25} are in the vapor phase. A quick transformation of B (~20-40 minutes) to form boron-rich boride according to following reaction suggests that the reaction kinetics are favorable.

$$2Mg\,(g) + 25B(s) \rightarrow Mg_2B_{25}(s) \quad (I)$$

When a B particle reacts with Mg vapor, the Mg_2B_{25} phase initially forms on the surface of boron particle (Figure 3, Stage 1), as shown in Figure 9. At this stage, an element of Mg_2B_{25} at the periphery of B particle experiences compressive tangential stresses. This is primarily because B (molar volume (V_B)=4.7 cm^3) particle (in equation I) undergoes volume expansion after transforming into Mg_2B_{25} (molar volume (V_{Mg2B25}=129.7 cm^3)) according to (I). The peripheral region is pushed away from the centre upon subsequent growth of the Mg_2B_{25} layer, unloads elastically and then experiences tensile tangential stress as illustrated schematically in Figure 9. This stress leads to the initiation of a radial crack due to the negligible plasticity of Mg_2B_{25}.[17] This phenomenon has been observed previously and reported as "Lithiation induced fracture" within the context of the diffusion of lithium in silicon particles.[17-21]

When elastic strain is small compared to reaction induced strain (volume strain: 11%), radial (σ_r), and tangential (σ_θ) stresses at any distance R from centre of a spherical β-B particle upon formation of thin Mg_2B_{25} shell can be described as;[17]

$$\sigma_r = -2\sigma_y \log\left(\frac{b}{r}\right) \quad (1)$$

$$\sigma_\theta = \sigma_y - \sigma_y \log\left(\frac{b}{r}\right)(a \le R \le b) \quad (2)$$

where b is the outer radius of sphere and a is the radius of an unreacted β-B sphere.

b is also expressed as a function of initial radius of particle prior to reaction (b_i) as

$$b = [a^3 + \beta(b_i^3 - a^3)]^{1/3} \quad (3)$$

The above equation takes relative volume expansion β (ratio of molar volume of Mg_2B_{25} to β-B) into consideration. The hoop stress is tensile in nature at the periphery (b=R) with a maximum value equal to the yield strength σ_y. Given the brittle nature of Mg_2B_{25}, hoop stress (σ_Θ=σ_y) is likely to initiate fracture of particle by generation of a crack.[12] It is noted that residual stresses can

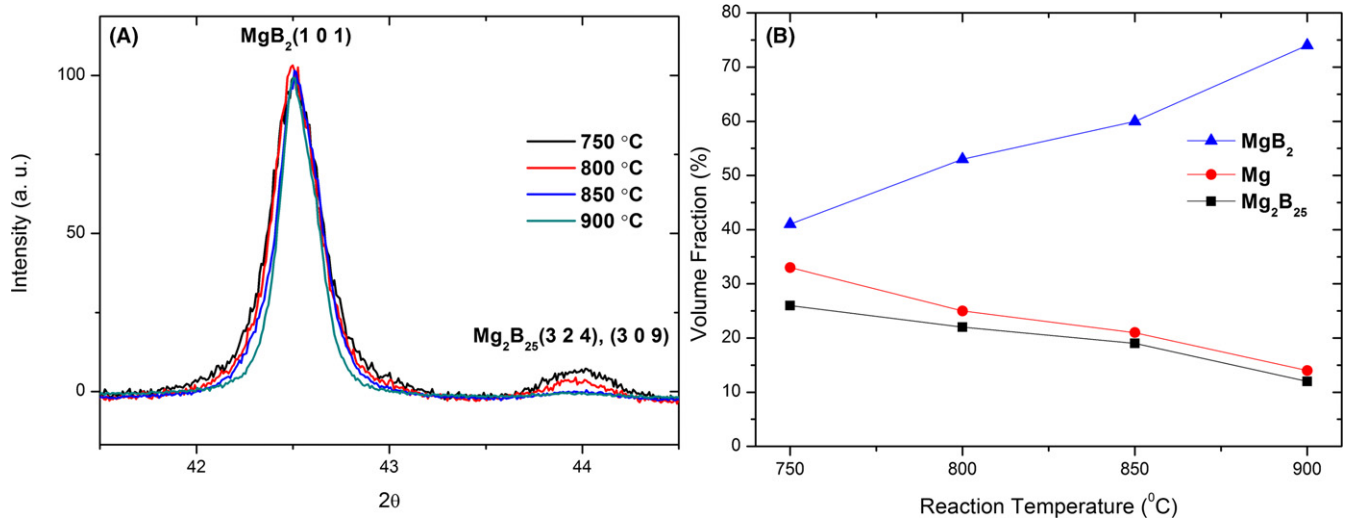

FIGURE 7 A, XRD patterns of samples reacted for 4 h at 750°C, 800°C, 850°C, and 900°C. Note that changing the relative amount of MgB_2 and Mg_2B_{25} phases varies depending on the temperature. B, Estimated volume fraction phases (MgB_2, Mg and Mg_2B_{25}) as a function of reaction temperature

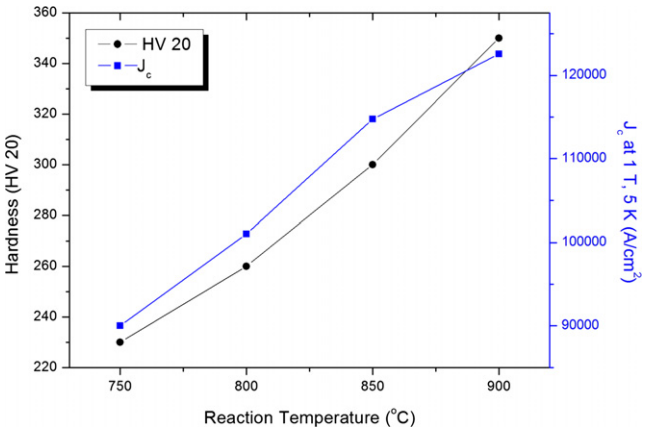

FIGURE 8 Variation of critical current density and hardness plotted as a function of reaction temperature

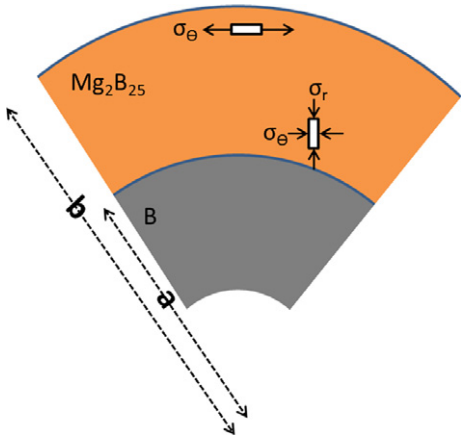

FIGURE 9 Schematic illustration of a progressing Mg_2B_{25} front and the generation of stress

remain compressive in a particle with flat surface. Thus, curvature is critical for the initiation of cracks at the surface of a particle.

This stress σ_y ($>\sigma_c$) would propagate the crack[17] if crack size is such that

$$G = Z\frac{\sigma_c^2}{E}b \tag{4}$$

where σ_c is the critical stress required to propagate a crack of length $2b$, Z is a geometrical factor, E is elastic modulus of Mg_2B_{25}, and G is the energy release rate. Although σ_y is clearly sufficiently high to propagate a crack for a short distance (as apparent from Figure 5A), the cracks do not propagate freely inwards since the tensile hoop stress decreases steadily, eventually becoming compressive toward the center.[17,21]

Energy-dispersive X-ray analysis at locations 1 and 2 in Figure 1D confirms the Mg_2B_{25} phase formation and the corresponding EDAX patterns are shown in Figure 10. At this stage, a considerable amount of Mg has occupied the pores in the boron precursor. It is evident from Figure 2 that significant portion of B powder is transformed into Mg_2B_{25} within the first 20 minutes of soaking time and that no detectable amount of superconducting MgB_2 is observed. Several particles in the microstructure (Figure 1D), appearing dark in contrast indicated by red dashed circle, represent unreacted β-Boron particles with B/Mg ratio of 98 (eg location 2) that have not yet transformed into Mg_2B_{25}. The relatively lighter in contrast particles (location 1) are confirmed as Mg_2B_{25} particles. EDS analysis on several random points within such areas suggests a

B/Mg atomic ratio of 10 as opposed to an ideally expected ratio of 12.5. The slight underestimation of this ratio is attributed to the interaction volume of the penetrating electron beam, some of which probe Mg metal beneath the particle.

The Mg infiltration depth (χ_0) into the porous boron preform can be expressed by following Washburn's equation in the Stage 2 of the IG process,[22]

$$(\chi) = \left(\frac{r\gamma\cos\theta}{2\eta}\right)^{1/2} .t(0)^{1/2} \quad (5)$$

r, γ, θ, and η represent the radius of cylindrical porous channels, surface tension, wetting angle between β-B(s)-Mg(l), and viscosity of Mg melt, respectively, whereas χ and t represent infiltration depth and time taken. Since weight gain is directly proportional to χ, equation 5 suggests a parabolic dependence of weight gain (dotted line in Figure 4) with time. A deviation from Washburn's model is expected in the present case as the pores are of irregular shapes and sizes. Moreover, other mechanisms, such as gravity, hydrostatic fluid pressure and negative pressure (from volume shrinkage in MgB_2 phase formation), are also expected to contribute to the uptake of Mg. The predicted and measured weight gain with reaction time is compared in Figure 4. Note that due to the unknown contact angle (θ), Washburn infiltration is assumed to reach completion after 1 hour, and weight gain from 0 to 1 hour is predicted. Li et al. observed that, at 675°C, Mg infiltrates to a depth of 40 μm in 1 hour in MgB_2 wires synthesized from nano-boron powder. Even after suitable correction for pore radius (assumed proportional to particle size), and a small change in viscosity, the rate of Mg uptake appears much more rapid in this study. It is therefore suggested that aside from liquid infiltration and other aforementioned mechanisms, vapor diffusion could also be another mode of transport of Mg from liquid reservoir since Mg is known for its high vapor pressure. The vapor diffusion process explains the observed phase transformation of B into Mg_2B_{25} everywhere within the sample and the absence of Mg phase in initial 20 minutes of the process. During this period, Mg atoms are adsorbed everywhere on β-B particle surface and react according to (I) to form Mg_2B_{25}, creating further driving force for Mg vapor influx. Mg pick up from classical Washburn liquid infiltration is likely to be limited to the edges of sample during initial 20 minutes of the soaking period.

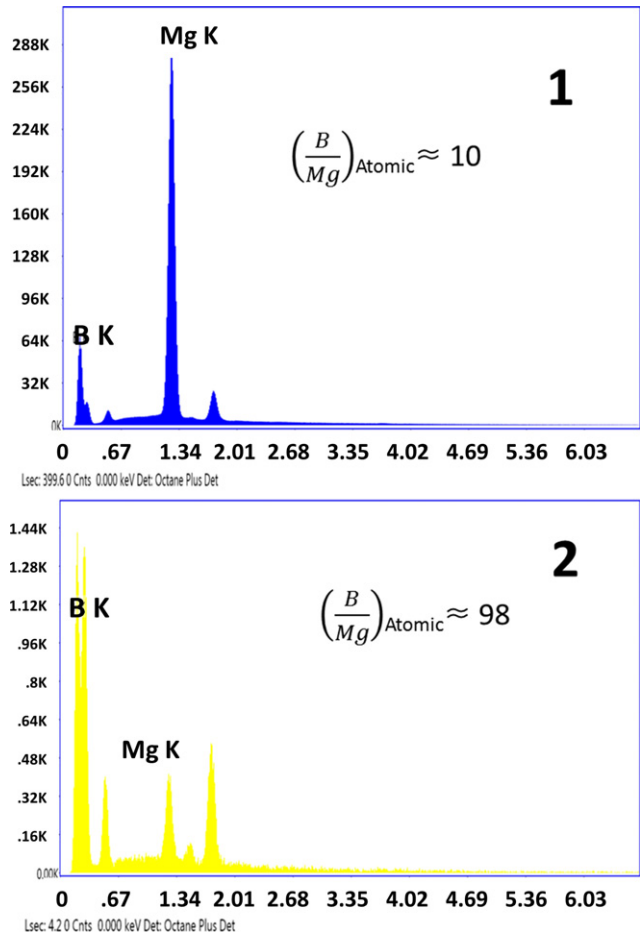

FIGURE 10 EDS point analysis on spots 1 and 2 (from Figure 1D) showing relative amounts of B and Mg

In the third and final stage of the process, the propagation of cracks, formation of a MgB_2 diffusion layer and sintering all occurred simultaneously. Mg(l) entered the cracks and reacted with Mg_2B_{25} at the crack tip/surface to form MgB_2. This chemical reaction can be expressed as;

$$2Mg_2B_{25}(s) + 21Mg(l) \rightarrow 25MgB_2(s) \quad (II)$$

Volumetric strain experienced at the crack tip by Mg_2B_{25} element can be described as

$$\varepsilon_V = \frac{2V_m^{Mg_2B_{25}} - 25V_m^{MgB_2}}{2V_m^{Mg_2B_{25}}} \sim 70\% \quad (6)$$

where V_m is molar volume, and ε_V and ε_L are volumetric and linear strains, respectively. Under the isotropic volume expansion, the linear strain ε_L is given by,

$$\varepsilon_L = \frac{\varepsilon_v}{3} \sim 23\% \quad (7)$$

Thus, the stress at the tip of the crack is given as[23]

$$\sigma_{cracktip} = E_{MgB_2}\varepsilon_L \sim 65GPa \quad (8)$$

Although such a volume expansion ahead of the crack tip is expected to blunt the tip and hinder crack propagation, as in the case of yttria-stabilized zirconia,[24,25] experimental evidence suggests that continuous formation of MgB_2 can impart stress larger than the one that can be sustained

elastically by Mg_2B_{25}. Therefore, the crack propagates further exposing fresh Mg_2B_{25} to Mg(l). DeFaw et al. also observed such time-dependent crack growth in MgB_2 synthesis from boron fibers.[9] As a result, cracks propagate radially inward, often resulting in the fragmentation of particles. Formation and propagation of these cracks play a vital role in formation of MgB_2 channels passing through the nonsuperconducting Mg_2B_{25} phase. This provides an added supercurrent path in the fully processed bulk material.

MgB_2 phase formation closely resembles a peritectic reaction where reaction occurs only on the surface and is governed by diffusion of various chemical species. Therefore, the reaction does not often reach completion, as is observed frequently in the fabrication of (RE)BCO superconductors, where the final microstructure invariably contains a considerable amount of unreacted phase (Y-211).[26,27] A decrease in Mg_2B_{25} phase content (12%) is observed as a result of Mg(l) reaction with Mg_2B_{25} phase and enhanced kinetics at higher temperature. Similarly, XRD patterns (Figure 7A) also show a diminishing phase content of Mg_2B_{25} with increasing reaction temperature. It is also worth noting that MgB_2 formed at lower temperature is "dirtier", as indicated by broader peaks in samples reacted at low temperature.

The so-called Deal and Grove model has been adopted to describe the Mg diffusion process in the growth of MgB_2.[28,29] In this model, it is assumed that all boron particles are spherical and of equal diameter, and that the diffusion process is a steady state. It is assumed that no reaction has taken place while Mg(l) occupies all the porous sites in the precursor.

According to Fick's first law,

$$J_{\mathrm{Mg}} = D\frac{C_{\mathrm{Mg-MgB_2}} - C_{\mathrm{MgB_2-Mg_2B_{25}}}}{x} \tag{9}$$

where D is the diffusivity of Mg in MgB_2, $C_{\mathrm{Mg\text{-}MgB2}}$ represents the concentration at Mg-MgB_2 interface, $C_{\mathrm{MgB2\text{-}Mg2B25}}$ is the Mg concentration at MgB_2-Mg_2B_{25} interface, J_{Mg} is influx of Mg atoms, and x is thickness of the MgB_2 layer.

For mass balance, the influx of Mg (J_{Mg}) should be equal to the rate of MgB_2 formation given that the number of moles of Mg diffusing through the MgB_2 layer is the same as that reacting with Mg_2B_{25} to form MgB_2. Assuming a first-order reaction,

$$J_{\mathrm{Mg}} = KC_{\mathrm{MgB_2-Mg_2B_{25}}} \tag{10}$$

where K is reaction constant in Equation 10.

Combining equations (9) and (10) yields

$$C_{\mathrm{MgB_2-Mg_2B_{25}}} = \frac{DC_{\mathrm{Mg-MgB_2}}}{D + xK} \tag{11}$$

$$J_{\mathrm{Mg}} = \frac{K(DC_{\mathrm{Mg-MgB_2}})}{D + xK} \tag{12}$$

Assuming that the MgB_2 layer grows by an infinitesimally small length dx in time dt, the number of moles of Mg crossing a unit cross-sectional area in dt is therefore J_{Mg}dt. These are number of Mg atoms reacting to form MgB_2 with volume of cuboid equaling unit area and length dx $\left(V_{Mg}^{MgB_2}\right)$ Note that 21 moles of Mg are required to form 25 moles of MgB_2. (equation II)

$$21J_{\mathrm{Mg}}\mathrm{d}t = 25V_{\mathrm{Mg}}^{\mathrm{MgB_2}} \quad \mathrm{d}x \tag{13}$$

$$\mathrm{d}t = \frac{25(D + xK)}{21KDC_{\mathrm{Mg-MgB_2}}} \quad V_{\mathrm{Mg}}^{\mathrm{MgB_2}}\mathrm{d}x \tag{14}$$

Invoking the assumption that the overall reaction is controlled by diffusion rather than reaction rates, equation (14) yields

$$\int_{t=0}^{t=t^*} \mathrm{d}t = \frac{25V_{\mathrm{Mg}}^{\mathrm{MgB_2}}}{21} \int_{x=0}^{x=20\times10^{-6}} \left(\frac{x}{DC_{\mathrm{Mg-MgB_2}}}\right)\mathrm{d}x \tag{15}$$

where t^* is the time necessary to complete reaction II (stage 3) at 900°C. The upper limit of x is chosen as the radius of the reacting particle. Values of D=10^{-14} m^2/s (900°C),[9] $C_{\mathrm{Mg\text{-}MgB2}}$=$6.6\times10^4$ $mol/m^{3,}$ yields t^*=6 hours $V_{Mg}^{MgB_2}$ = 5.6×10^4 mol/m^3. Similarly, to ensure completion of reaction at 900°C at 4 hours (When time taken for completion of stage 1 and 2 ~ 1 hours), a uniform particle size of ~14 μm would be required for this process.

As the MgB_2 layer forms on the surface of particle, it almost doubles in volume, leading to impingement of particles on one another. A large contact area between the particles presents clear evidence of sintering between the particles.[6] Critical current density is essentially a function of MgB_2 phase fraction and degree of sintering between the particles. These two factors together form A_f, the effective cross-sectional area[30]. Therefore, J_c increases almost linearly with the reaction temperature, as expected. Similarly, it can be argued that bulk hardness (HV20) is a strong function of sintering and individual phase fraction.[31,32] Thus an observed increase in hardness of these samples with temperature gives another independent evidence of sintering between the MgB_2 particles.

5 | CONCLUSION

It can be concluded that MgB_2 phase formation in IG process is a three stage process that can be summarized by the following chemical equations.

$$4Mg(g) + 50B(s) \rightarrow 2Mg_2B_{25}(s)$$

$$2Mg_2B_{25}(s) + 21Mg(l) \rightarrow 25MgB_2(s)$$

With the formation of intermediate phase Mg_2B_{25} and associated volume expansion, cracks were initiated in all boron particles. These cracks propagated radially inwards, originating from crack tip stresses, resulting fracture and disintegration in a number of particles, and thereby offering better kinetics by exposing large surface area for reaction. Mg infiltration in the precursor was rapid, aided probably by vapor phase transport. This was followed by MgB_2 layer growth, limited by diffusion of Mg atoms, and simultaneous sintering together to form grain boundaries. Despite reaction at high temperature (900°C, 4 hours), the samples contained residual intermediate boride. Therefore, an optimized particle size, of sufficient size to create pore geometries to facilitate Mg(l) infiltration, yet small enough to ensure complete diffusion of Mg atoms to the center and to provide grain-boundary pinning, could be the way forward for the fabrication of high-performance IG processed MgB_2 bulk superconductors.

ACKNOWLEDGMENT

Authors acknowledge financial support from KACST-Cambridge Joint Centre of Excellence in Advanced Materials and Manufacturing (CAMM) based at the University of Cambridge, UK. Partial financial support from Engineering and Physical Sciences Research Council, UK (Grant: EP/K031422/1) is gratefully acknowledged.

REFERENCES

1. Nagamatsu J, Nakagawa N, Muranaka T, Zenitani Y, Akimitsu J. Superconductivity at 39 K. *Nature*. 2001;410:63-64.
2. Kambara M, Hari Babu N, Sadki ES, et al. High intergranular critical currents in metallic MgB_2 superconductor. *Supercond Sci Technol*. 2001;14:L5-L7.
3. Bhagurkar AG, Yamamoto A, Hari Babu N, Dennis AR, Durrell JH, Cardwell DA. Synthesis of dense bulk MgB_2 by infiltration and growth. *Supercond Sci Technol*. 2015;28:015012-015018.
4. Giunchi G. High density MgB_2 obtained by reactive liquid Mg infiltration. *Int J Mod Phys B*. 2003; 17:453-461.
5. Giunchi G, Ripamonti G, Cavallin T, Bassani E. The reactive liquid Mg infiltration process to produce large superconducting bulk manufacts. *Cryogenics*. 2006;46:237-242.
6. Bhagurkar AG, Yamamoto A, Anguilano L, et al. A trapped magnetic field of 3 T in homogeneous bulk MgB_2 superconductors fabricated by modified precursor infiltration and growth process. *Supercond Sci Technol*. 2016;29:035008-035016.
7. Giunchi G, Albisetti AF, Malpezzi L, Saglietti L, Perini E. High Performance bulk MgB2 obtained by the Reactive Mg-Infiltration Process: New Advancements and Solutions, Proceedings of 2011 IEEE International Conference on Applied Superconductivity and Electromagnetic Devices, 2011; 313-317.
8. Naito T, Ogino A, Fujishiro H. Potential ability of 3 T class trapped field on MgB2 bulk surface synthesized by the infiltration capsule method. *Supercond Sci Technol*. 2016;29:115003-115009.
9. DeFouw JD, Dunand DC. Mechanism and kinetics of MgB_2 synthesis from boron fibers. *Acta Mater*. 2008;56:5751-5763.
10. Albisetti AF, Saglietti L, Perini E, Schiavone C, Ripamonti G, Giunchi G. The Mg_2B_{25} formation and its role in the preparation of bulk MgB_2 superconductors. *Solid State Sci*. 2012;14:1632-1635.
11. Li GZ, Sumption MD, Collings EW Kinetic analysis of MgB_2 layer formation in advanced internal magnesium infiltration processed MgB_2 wires. *Acta Mater*, 2015;96.
12. Aarstad K. Protective films on molten Mg, PhD Thesis, Norwegian University of Science and Technology 2004.
13. Bhagurkar AG, Hari Babu N, Dennis AR, Durrell JH, Cardwell DA Characterization of bulk MgB_2 synthesized by Infiltration and Growth. *IEEE Trans Appl Supercond*. 25:6801504-6801508.
14. Chen DX, Goldfarb RB. Kim model for magnetization of type-II superconductors. *J Appl Phys*. 1989;66:2489-2500.
15. Giunchi G, Orecchia C, Malpezzi L, Masciocchi N. Analysis of minority crystalline phases in bulk superconducting MgB_2 obtained by reactive liquid Mg infiltration. *Physica C*. 2006;433:182-188.
16. Giunchi G, Malpezzi L, Masciocchi N. A new crystalline phase of the boron-rich metal-boride family: the Mg_2B_{25} species. *Solid State Sci*. 2006;8:1202-1208.
17. Zhao K, Pharr M, Wan Q, et al. Concurrent reaction and plasticity during initial lithiation of crystalline silicon in lithium ion batteries. *J Electrochem Soc*. 2012;159:A238-A243.
18. Liu XH, Zhong L, Huang S, Mao SX, Zhu T, Huang JY. Size dependent fracture of silicon nanoparticles during lithiation. *ACS Nano*. 2012;6:1522-1531.
19. McDowell MT, Lee SW, Nix WD, Cui Y. Understanding the lithiation of silicon and other alloying anodes for lithium ion batteries. *Adv Mater*. 2013;25:4966-4985.
20. Ebner M, Marone F, Stampanoni M, Wood V. Visualization and quantification of electrochemical and mechanical degradation in Li ion batteries. *Science*. 2013;342:716-720.
21. Huang S, Fan F, Li J, Zhang S, Zhu T. Stress generation during lithiation of high capacity electrode particles in lithium ion batteries. *Acta Mater*. 2013;61:4354-4364.
22. Washburn EW. The dynamics of capillary flow. *Phys Rev B*. 1921;17:273-283.
23. Nesterenko VF, Gu Y. Elastic properties of hot-isostatically pressed magnesium diboride. *Appl Phys Lett*. 2003;82:4104-4106.
24. Yanagida H, Koumoto K, Miyayama M. *The Chemistry of Ceramics*. Hoboken, NJ, John Wiley & Sons; 1996.
25. Portert DL, Heuer AH. Mechanism of toughening partially stabilized zirconia (PSZ). *J Am Ceram Soc*. 1977;60:183-184.
26. Iida K, Hari Babu N, Shi Y, Cardwell DA. Seeded infiltration and growth of large, single domain Y-Ba-Cu-O bulk superconductors with very high critical current densities. *Supercond Sci Technol*. 2005;18:1421-1427.

27. Hari Babu N, Shi Y, Iida K, Cardwell DA. A practical route for the fabrication of large single crystal Re-Ba-Cu-O superconductors. *Nat Mater* 2005;4:476-480.
28. Deal BE, Grove AS. General relationship for thermal oxidation of silicon. *J Appl Phys*. 1965;36:3770-3778.
29. Kim HM, Yim SS, Kim KB, Moon SH, Kim YW, Kang DH. Growth kinetics of MgB_2 layer and interfacial MgO layer during ex situ annealing of amorphous boron film. *J Mater Res*. 2004;19:3081-3089.
30. Rowell JM. The widely variable resistivity of MgB_2 samples. *Supercond Sci Technol*. 2003;16:R17-R27.
31. Mukhopadhyay AK, Datta SK, Chakraborty D. Hardness of silicon nitride and sialon. *Ceram Int*. 1991;17:121-127.
32. Dancer CEJ, Mikheenko P, Bevan A, Abell JS, Todd RI, Grovenor CRM A study of the sintering behaviour of magnesium diboride. *J Eur Ceram Soc*. 2009; 29:1817-1824.

How to cite this article: Bhagurkar AG, Yamamoto A, Dennis AR, et al. Microstructural evolution in infiltration-growth processed MgB_2 bulk superconductors. *J Am Ceram Soc*. 2017;00:1–10.